HHS Public Access

Author manuscript

ChemNanoMat. Author manuscript; available in PMC 2018 January 01.

Published in final edited form as:

ChemNanoMat. 2017 January ; 3(1): 17–21. doi:10.1002/cnma.201600258.

Chirality Controls Reaction-Diffusion of Nanoparticles for Inhibiting Cancer Cells

Xuewen Du[a], **Jie Zhou**[a], **Jiaqing Wang**[a], **Rong Zhou**[a], and **Prof. Dr. Bing Xu**[a]

[a]Department of Chemistry, Brandeis University, 415 South St. Waltham, MA 02454 (USA)

Abstract

Reaction-diffusion (RD) is the most important inherent feature of living organism, but it has yet to be used for developing biofunctional nanoparticles (NPs). Here we show the use of chirality to control the RD of NPs for selectively inhibiting cancer cells. We observe that L-phosphotyrosine (L-pY) decorated NPs (NP@L-pYs) are innocuous to cells, but D-pY decorated ones (NP@D-pYs) selectively inhibit cancer cells. Our study shows that alkaline phosphatases (ALP), presented in the culture and overexpressed on the cancer cells, dephosphorylates NP@L-pYs much faster than NP@D-pYs. Such a rate difference allows the NP@D-pYs to be mainly dephosphorylated on cell surface, thus adhering selectively on the cancer cells to result in poly(ADP-ribose)polymerase (PARP) hyperactivation mediated cell death. Without phosphate groups or being prematurely dephosphorylated before reaching cancer cells (as the case of NP@L-pYs), the NPs are innocuous to cells. Moreover, NP@D-pYs even exhibit more potent activity than cisplatin for inhibiting platinum-resistant ovarian cancer cells (e.g., A2780-cis). As the first example of chirality controlling RD process of NPs for inhibiting cancer cells, this work illustrates a fundamentally new way for developing nanomedicine based on RD processes and nanoparticles.

Entry for the Table of Contents

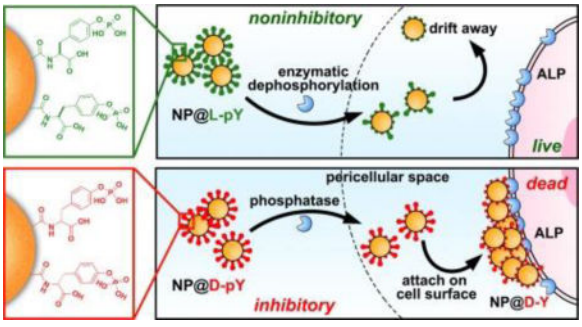

This work reports the use of chirality to control the RD of NPs for selectively inhibiting cancer cells. The different dephosphorylation rates of the NP@D-pYs and NP@L-pYs allow NP@D-pYs to be mainly dephosphorylated on cell surface, thus adhering selectively on the cancer cells to result in PARP hyperactivation mediated cell death.

Correspondence to: Bing Xu.

Dedication

Keywords

Reaction-diffusion; nanoparticles; cancer cell inhibition; chirality; phosphatases

A common strategy in the development of nanomedicines is to attach ligands or antibodies to nanoparticles (NPs) for specifically targeting proteins or cells, thus achieving the goal of diagnostics or therapy or both.[1] However, due to genomic instability of cancer cells, mutation often occurs,[2] thus resulting in the loss of the affinity of the antibody to the cancer cells. Moreover, the *in vivo* stability of antibodies varies, which may contribute to the low efficacy of delivery of NPs for cancer therapy.[3] These inherent drawbacks associated with the loss of specific ligand-receptor interactions or the lack of biostability of antibodies underscores a genuine need of novel approaches for developing nanomedicines to target cells without solely relying on the tight and specific antibody binding. Based on the integration of enzymatic reaction and molecular self-assembly,[4] we and others are developing enzyme-instructed self-assembly (EISA) as a new approach for selectively inhibiting[5] or imaging[6] cancer cells. The successful use of EISA to inhibit cancer cells[7] validates the concept of using a multistep process[5]—that is, enzymatic reaction and assembly—for targeting cancer cells. We have applied the concept of EISA to magnetic NPs, and our results show that the D-phosphotyrosine (D-pY) decorated magnetic NPs (NP@D-pYs) selectively capture cancer cells upon the dephosphorylation by the ALPs overexpressed on the surface of cancer cells.[8] To our surprising, when we replaced the D-pY by L-phosphotyrosine (L-pY), we find that the L-pY decorated NPs (NP@L-pYs) are unable to capture cancer cells. This unexpected result leads to this work, which explores the roles of chirality of NPs during EISA for inhibiting cancer cells.

In this work, our studies reveal that alkaline phosphatases (ALPs) dephosphorylate the NP@L-pYs eight times faster than that of NP@D-pYs, which allows most of the NP@L-pYs to be converted to NP@L-Ys in culture medium before reaching cells. On the contrary, most of the NP@D-pYs undergo dephosphorylation on the surface of cancer cells that overexpress ALPs. Such in-situ dephosphorylation contributes to the adhesion of NP@D-Ys on cancer cells to inhibit the cells. Moreover, preliminary mechanistic examination reveals that NP@D-Ys, being generated by the enzymatic reactions, adhere strongly on the cell surface and likely activate the extrinsic cell death pathway to result in PARP hyperactivation mediated cell death. Moreover, this reaction-diffusion (RD) process effectively and selectively inhibits cancer cells in the co-culture of cancer cells (HeLa-GFP) and stromal cells (HS-5). In addition, this process is general for inhibiting other cancer cells, including drug-resistant ones (e.g., T98G, MES-SA, and A2780-cis cells). Considering that RD is the most important inherent feature of living organism,[9] this work is significant because it, for the first time, illustrates a facile approach that uses chirality to control the RD of NPs for targeting cancer cells.

After synthesizing the NP@L-pYs and NP@D-pYs using the reported procedure,[8] we examined them by transmission electron microscopy (TEM). As shown by TEM (Figure S1), after being modified by L-pY or D-pY, these two types of NPs exhibit well-defined iron oxide cores and amphiphilic coatings. Having the total diameter of around 10 nm, the

NP@D-pYs (or NP@L-pYs) slightly cluster to form small aggregates with an average size of 500 nm. The quantification of the phosphate group on NP@L-pYs and NP@D-pYs indicates that, on average, there are around 115 phosphotyrosine molecules on NP@L-pYs, and 104 molecules on NP@D-pYs.[10]

After the characterization of NP@L-pYs and NP@D-pYs, we examine their activities for inhibiting cancer cells. Because NP@D-pYs inhibit the growth of cancer cells effectively, with the IC_{50} of 14 μg/mL and IC_{90} of 45 μg/mL against the HeLa-GFP cells,[8] we incubate the NP@D-pYs with several other human cancer cells using cell assays. As shown in Figure 2A and Figure S2, NP@D-pYs inhibit T98G (glioblastoma) at the IC_{50} of 13 μg/mL and IC_{90} of 29 μg/mL. Moreover, the NP@D-pYs show high inhibition efficiency toward two multidrug resistant (MDR) cancer cells, such as MES-SA/Dx5 (uterine sarcoma) and A2780-cis (ovarian carcinoma), having the IC_{50} of 18 or 17 μg/mL against MES-SA/Dx5 or A2780-cis cells, respectively. However, the NPs decorated with D-tyrosine (NP@D-Ys) show little cytotoxicity to all these cancer cells (Figure S3). This result indicates that the in-situ dephosphorylation of NP@D-pYs, similar to the EISA of small molecules,[6–7, 7c, 8] is critical for inhibiting the cancer cells. Based on the above results, we reckoned that NP@L-pYs should inhibit cancer cells because ALPs on cancer cells surface should dephosphorylate the L-pYs attached on the NP@L-pYs, which would result in the subsequent assembly of NP@L-Ys on cancer cell surface to inhibit the cancer cells. Unexpectedly, the NP@L-pYs are innocuous to cancer cells. As shown in Figure 2B and Figure S4, NP@L-pYs have the IC_{50} value larger than 50 μg/mL against all the four cancer cell lines (HeLa-GFP, T98G, MES-SA/Dx5, A2780-cis cells). Optical microscopy reveals that the cancer cells treated with NP@D-pYs differ from the cancer cells treated by NP@L-pYs (Figure 2C and Figure S6). While few NP@L-Ys cover the cancer cell surface, a lot of NP@D-Ys adhere on the cancer cell surface, as depicted in Figure 2C.

Because both NP@L-Ys and NP@D-Ys are innocuous to cells (Figure S3, S5), cell death unlikely results from that NP@D-Ys bind tighter to the cancer cells than NP@L-Ys do. Considering that the different chirality of L-pY and D-pY may result in different rate of dephosphorylation catalyzed by ALPs, we compare the dephosphorylation rate of these two types of NPs (Figure S7). As shown in Figure 3A, in the conditioned culture medium that contains secreted enzymes, the dephosphorylation rate of NP@L-pYs is much higher than that of NP@D-pYs, with the dephosphorylation half time ($t_{1/2}$) to be 10.4 or 85.1 h for NP@L-pYs or NP@D-pYs, respectively. This result indicates that secreted enzymes by cancer cells can dephosphorylate NP@L-pYs about eight times faster than NP@D-pYs. Thus, it is likely that most of L-pYs on the NP@L-pYs would be dephosphorylated before they reach the cancer cells. So NP@L-pYs are innocuous to cells. In the case of NP@D-pYs, because of the slow dephosphorylation of NP@D-pYs in the culture medium and the overexpression of ALPs on cancer cells, most of the NP@D-pYs turn to NP@D-Ys on the cancer cell surface, thus adhering and inhibiting the cancer cells. Moreover, we also quantify the remaining phosphate groups on the NPs by incubating the NPs with cancer cells for 12 h (Figure 3B). Our results reveal that there are still around 18% of phosphates left on NP@D-pYs, but only 2% of phosphate groups remaining on NP@L-pYs under the same condition. This result implies that the remaining phosphates on NP@D-pYs may contribute to the adhesion of the NPs to the cells since NP@D-Ys, by themselves, hardly adhere to cells.[8]

To further validate that the ALPs overexpressed on cancer cells catalyze the conversion of NP@D-pYs to NP@D-Ys to cause cell death, we add exogenous ALP into to the cell culture and find that the addition of ALP (5 U/mL) significantly reduces the inhibitory activity of NP@D-pYs against the four cell lines (i.e., increasing the IC_{50} value of NP@D-pYs against cancer cells, Figure 4A). Moreover, the addition of the uncompetitive inhibitor of placental ALP (i.e., L-Phe, 5 mM)[11] significantly decreases the inhibitory activity of NP@D-pYs (Figure 4B), indicating that ALPs dephosphorylate NP@D-pYs on cancer cells to contribute to the cell death. All the above results indicate that NP@D-pYs, having a relatively slow dephosphorylation rate, undergo EISA locally on cancer cells, thus inhibiting cancer cells. On the contrary, NP@L-pYs, having a fast dephosphorylation rate, fail to localize on cancer cells, thus remaining largely innocuous. In other word, chirality dictates the RD of the NPs (i.e., NP@D-pYs) for targeting the cancer cells (Figure 1).

To understand the mode of the cell death caused by the assembly of NPs, we incubate HeLa-GFP cells with the NP@D-pYs and several inhibitors related to cell death pathways. As shown in Figure 4C, zVAD-fmk (45 μM),[12] an apoptosis inhibitor, increases the viability of the HeLa-GFP cells treated with NP@D-pYs (20 μg/mL) from 41% to 65%, Moreover, the addition of necrostatin-1 (50 μM),[13] a necroptosis inhibitor, is also able to protect cells from NP@D-pYs, increasing the cell viability from 41% to 61%. These results indicate that the NP@D-pYs induce cell death via two related cell death pathways, apoptosis and necroptosis.[14] Two kinds of PARP inhibitors (i.e., 3-aminobenzamide[15] or PJ34[16]) almost completely abrogate the cell inhibition (Figure S8), indicating that the aggregates of NP@D-Ys on cancer cells cause cell death via PARP hyperactiviation (a downstream event in cell death signaling pathway[17]). Moreover, the addition of tetramisole, an inhibitor of tissue nonspecific ALP (TNAP),[18] increases the cell viability against NP@D-pYs from 41% to 65%, confirming that TNAP on HeLa-GFP cells also dephosphorylates NP@D-pYs to cause cell death, agreeing with that L-Phe only partially protects the HeLa-GFP cells from ND@D-pYs. Contrasting to the case of NP@D-pYs, all these inhibitors have little effect on the cancer cells treated with NP@L-pYs (Figure 4D), agreeing with that NP@L-pYs are innocuous to the cells.

To further understand the mechanism of the cell death caused by the NPs on cancer cell surface, we use Western blotting to analyze the expression of several cell death signaling molecules because of the involvement of PARP in cell death caused by NP@D-pYs. As shown in Figure 5A, upon the treatment of NP@D-pYs, HeLa-GFP cells slightly increase the expressions of caspase-8, but the amount of cleaved caspase-8 rises drastically, agreeing with that some cells undergo apoptosis (Figure 4C). Moreover, the incubation of HeLa-GFP cells with NP@D-pYs also induces the expressions of cleaved caspase-3 and cleaved PARP, which is consistent with the cell viability study related to necrostatin-1 and PJ34, the inhibitors of RIP1 and PARP, respectively. NP@D-pYs also increase the expression of RIP1 more than NP@L-pYs do, agreeing with that some cells undergo necroptosis. In the case HeLa-GFP cells treated by NP@L-pYs, only a weak band of cleaved PARP appears at 24 h, while the expressions of other signal molecules are essentially the same as those of the controls (i.e., adding unmodified NPs and without adding NPs). We also use ELISA to quantify the amount of several key apoptosis signal molecules over time in the HeLa-GFP cells (Figure 5B). The results show that the amount of active caspase-3 and active PARP

begins to increase even after 4 h of treatment with NP@D-pYs, which is consistent with the Western blotting data, suggesting that the cells undergo caspase and PARP dependent cell death. However, the ELISA analysis shows that the expression level of p53 and phospho-Bad hardly change, indicating that the cell death unlikely involves intrinsic cell death signaling.[19] In addition, after the treatment with NP@L-pYs, the expressions of the key cell death signaling molecules largely remain constant over time (Figure 5C), which agrees with the Western blotting on the protein expressions of the cells treated by NP@L-pYs. These results agree with the distinct viabilities of the cells treated by NP@D-pYs and NP@L-pYs.

Considering the sizes of the NP may be critical for the adhesion, we attached D-pY to smaller magnetic NP (S-NP, 3 nm) and examine cytotoxic. We found the S-NP@D-pYs are much less toxic due to the low loading of D-pYs on the S-NP (Figure S9). Thus, the genuine size effect remains to be elucidated.

In conclusion, this work illustrates a new concept that chirality controls RD of NPs for inhibiting cancer cells. While the results lead us to speculate that some percentage of phosphates is needed for cell surface adhesion, the optimal range of the phosphate density likely would be cell specific. Because cells commonly employ membrane proteins and secreted proteins in complicated cellular milieu for controlling cellular functions, the concept illustrated by this work may be applicable to proteins or enzymes other than ALPs. In addition, this approach may be applicable for other nanostructures,[20] such as gold cages[21] or quantum dots.[22] While stereochemistry (i.e., chirality) has become a prominent guide principle for designing drugs based on tight ligand-receptor interactions, the use of stereochemistry to control multiple step process, such as RD processes, has received little attention, yet promise a new paradigm at the intersection of chemical kinetics, stereochemistry, and cell biology. Our future studies will focus on using other enzymes, such as MMP-9,[23] or designing NPs based on the expression of ALPs on cancer cells.

Supplementary Material

Refer to Web version on PubMed Central for supplementary material.

Acknowledgments

This work was partially supported by NIH (R01CA142746), NSF (MRSEC-1420382) and Keck Foundation. JZ is an HHMI international student fellow.

References

1. a) Na HB, Song IC, Hyeon T. Adv. Mater. 2009; 21:2133–2148.b) Gao JH, Gu HW, Xu B. Acc. Chem. Res. 2009; 42:1097–1107. [PubMed: 19476332] c) Seo D, Southard KM, Kim JW, Lee HJ, Farlow J, Lee JU, Litt DB, Haas T, Alivisatos AP, Cheon J, Gartner ZJ, Jun YW. Cell. 2016; 165:1507–1518. [PubMed: 27180907] d) You CC, Miranda OR, Gider B, Ghosh PS, Kim IB, Erdogan B, Krovi SA, Bunz UHF, Rotello VM. Nat. Nanotechnol. 2007; 2:318–323. [PubMed: 18654291] e) Murray CB, Kagan CR, Bawendi MG. Annu. Rev. Mater. Sci. 2000; 30:545–610.f) Sonnichsen C, Reinhard BM, Liphardt J, Alivisatos AP. Nat. Biotechnol. 2005; 23:741–745. [PubMed: 15908940] g) Nie SM, Emery SR. Science. 1997; 275:1102–1106. [PubMed: 9027306] h) Yang X, Yang MX, Pang B, Vara M, Xia YN. Chem. Rev. 2015; 115:10410–10488. [PubMed:

26293344] i) Ng KK, Zheng G. Chem. Rev. 2015; 115:11012–11042. [PubMed: 26244706] j) Du X, Zhou J, Shi J, Xu B. Chem. Rev. 2015; 115:13165–13307. [PubMed: 26646318]

2. a) Hollstein M, Sidransky D, Vogelstein B, Harris CC. Science. 1991; 253:49–53. [PubMed: 1905840] b) Reya T, Morrison SJ, Clarke MF, Weissman IL. Nature. 2001; 414:105–111. [PubMed: 11689955]
3. a) Jiang W, Kim BYS, Rutka JT, Chan WCW. Nat. Nanotechnol. 2008; 3:145–150. [PubMed: 18654486] b) Wilhelm S, Tavares AJ, Dai Q, Ohta S, Audet J, Dvorak HF, Chan WCW. Nat. Rev. Mater. 2016; 1:12.
4. a) Yang Z, Liang G, Xu B. Acc. Chem. Res. 2008; 41:315–326. [PubMed: 18205323] b) Yang ZM, Gu HW, Fu DG, Gao P, Lam JK, Xu B. Adv. Mater. 2004; 16:1440–1444.
5. Zhou J, Xu B. Bioconjugate Chem. 2015; 26:987–999.
6. Zhou J, Du X, Berciu C, He H, Shi J, Nicastro D, Xu B. Chem. 2016; 1:246–263. [PubMed: 28393126]
7. a) Kuang Y, Shi J, Li J, Yuan D, Alberti KA, Xu Q, Xu B. Angew. Chem. Int. Ed. 2014; 53:8104–8107.b) Huang P, Gao Y, Lin J, Hu H, Liao HS, Yan X, Tang Y, Jin A, Song J, Niu G, Zhang G, Horkay F, Chen X. ACS Nano. 2015; 9:9517–9527. [PubMed: 26301492] c) Pires RA, Abul-Haija YM, Costa DS, Novoa-Carballal R, Reis RL, Ulijn RV, Pashkuleva I. J. Am. Chem. Soc. 2015; 137:576–579. [PubMed: 25539667] d) Tanaka A, Fukuoka Y, Morimoto Y, Honjo T, Koda D, Goto M, Maruyama T. J. Am. Chem. Soc. 2015; 137:770–775. [PubMed: 25521540] e) Zhou J, Du X, Yamagata N, Xu B. J. Am. Chem. Soc. 2016; 138:3813–3823. [PubMed: 26966844]
8. Du X, Zhou J, Wu L, Sun S, Xu B. Bioconjugate Chem. 2014; 25:2129–2133.
9. Epstein IR, Xu B. Nat. Nanotechnol. 2016; 11:312–319. [PubMed: 27045215]
10. Du X, Zhou J, Xu B. J. Colloid Interface Sci. 2015; 447:273–277. [PubMed: 25586118]
11. Fishman WH, Inglis NI, Green S. Nature. 1963; 198:685–686. [PubMed: 13945318]
12. Jurgensmeier JM, Xie ZH, Deveraux Q, Ellerby L, Bredesen D, Reed JC. Proc. Natl. Acad. Sci. U.S.A. 1998; 95:4997–5002. [PubMed: 9560217]
13. Degterev A, Hitomi J, Germscheid M, Ch'en IL, Korkina O, Teng X, Abbott D, Cuny GD, Yuan C, Wagner G, Hedrick SM, Gerber SA, Lugovskoy A, Yuan J. Nat. Chem. Biol. 2008; 4:313–321. [PubMed: 18408713]
14. Ashkenazi A, Dixit VM. Science. 1998; 281:1305–1308. [PubMed: 9721089]
15. Kruman, Culmsee C, Chan SL, Kruman Y, Guo ZH, Penix L, Mattson MP. J. Neurosci. 2000; 20:6920–6926. [PubMed: 10995836]
16. Du XL, Matsumura T, Edelstein D, Rossetti L, Zsengeller Z, Szabo C, Brownlee M. J. Clin. Invest. 2003; 112:1049–1057. [PubMed: 14523042]
17. Yu SW, Wang HM, Poitras MF, Coombs C, Bowers WJ, Federoff HJ, Poirier GG, Dawson TM, Dawson VL. Science. 2002; 297:259–263. [PubMed: 12114629]
18. Sugawara Y, Suzuki K, Koshikawa M, Ando M, Iida J. Jpn. J. Pharmacol. 2002; 88:262–269. [PubMed: 11949880]
19. Datta SR, Dudek H, Tao X, Masters S, Fu HA, Gotoh Y, Greenberg ME. Cell. 1997; 91:231–241. [PubMed: 9346240]
20. a) Hu SH, Gao XH. J. Am. Chem. Soc. 2010; 132:7234–7237. [PubMed: 20459132] b) Liu J, Sun ZK, Deng YH, Zou Y, Li CY, Guo XH, Xiong LQ, Gao Y, Li FY, Zhao DY. Angew. Chem. Int. Ed. 2009; 48:5875–5879.c) Wang C, Daimon H, Onodera T, Koda T, Sun SH. Angew. Chem. Int. Ed. 2008; 47:3588–3591.d) Jun YW, Choi JS, Cheon J. Angew. Chem. Int. Ed. 2006; 45:3414–3439.e) Zhou C, Long M, Qin YP, Sun XK, Zheng J. Angew. Chem. Int. Ed. 2011; 50:3168–3172.f) Lin WB, Rieter WJ, Taylor KML. Angew. Chem. Int. Ed. 2009; 48:650–658.
21. Yavuz MS, Cheng YY, Chen JY, Cobley CM, Zhang Q, Rycenga M, Xie JW, Kim C, Song KH, Schwartz AG, Wang LHV, Xia YN. Nat. Mater. 2009; 8:935–939. [PubMed: 19881498]
22. a) Shen J, Zhao L, Han G. Adv. Drug Delivery Rev. 2013; 65:744–755.b) So MK, Xu CJ, Loening AM, Gambhir SS, Rao JH. Nat. Biotechnol. 2006; 24:339–343. [PubMed: 16501578]
23. Yang ZM, Ma ML, Xu B. Soft Matter. 2009; 5:2546–2548.

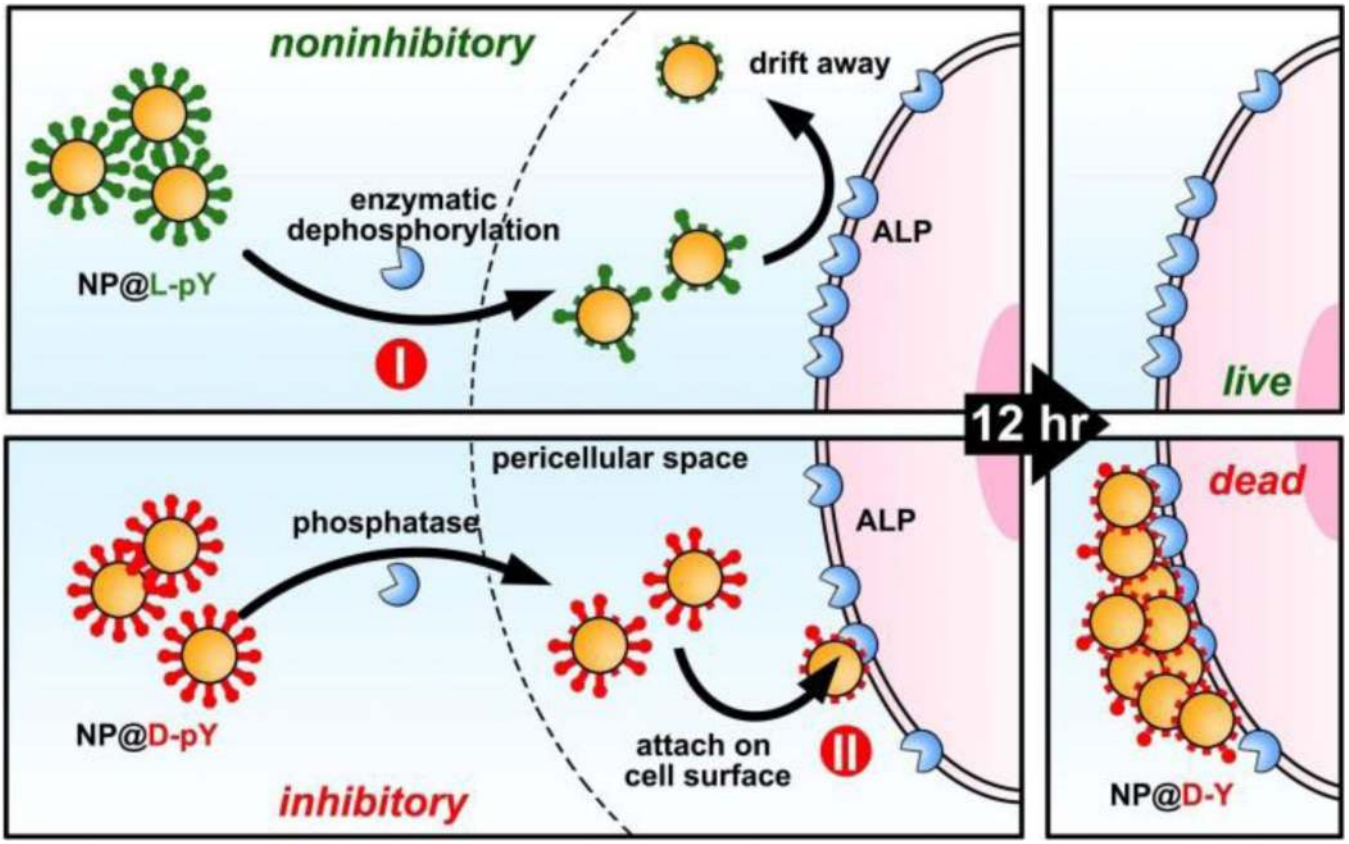

Figure 1.

Chirality of NPs controls RD to result in cell death. (I) The secreted enzymes in the culture medium dephosphorylate most of pYs on the NP@L-pYs. (II) The ALPs on cancer cell surface dephosphorylate most of pYs on NP@D-pYs, which enables the NP@D-Y to adhere to the cells and to cause cell death.

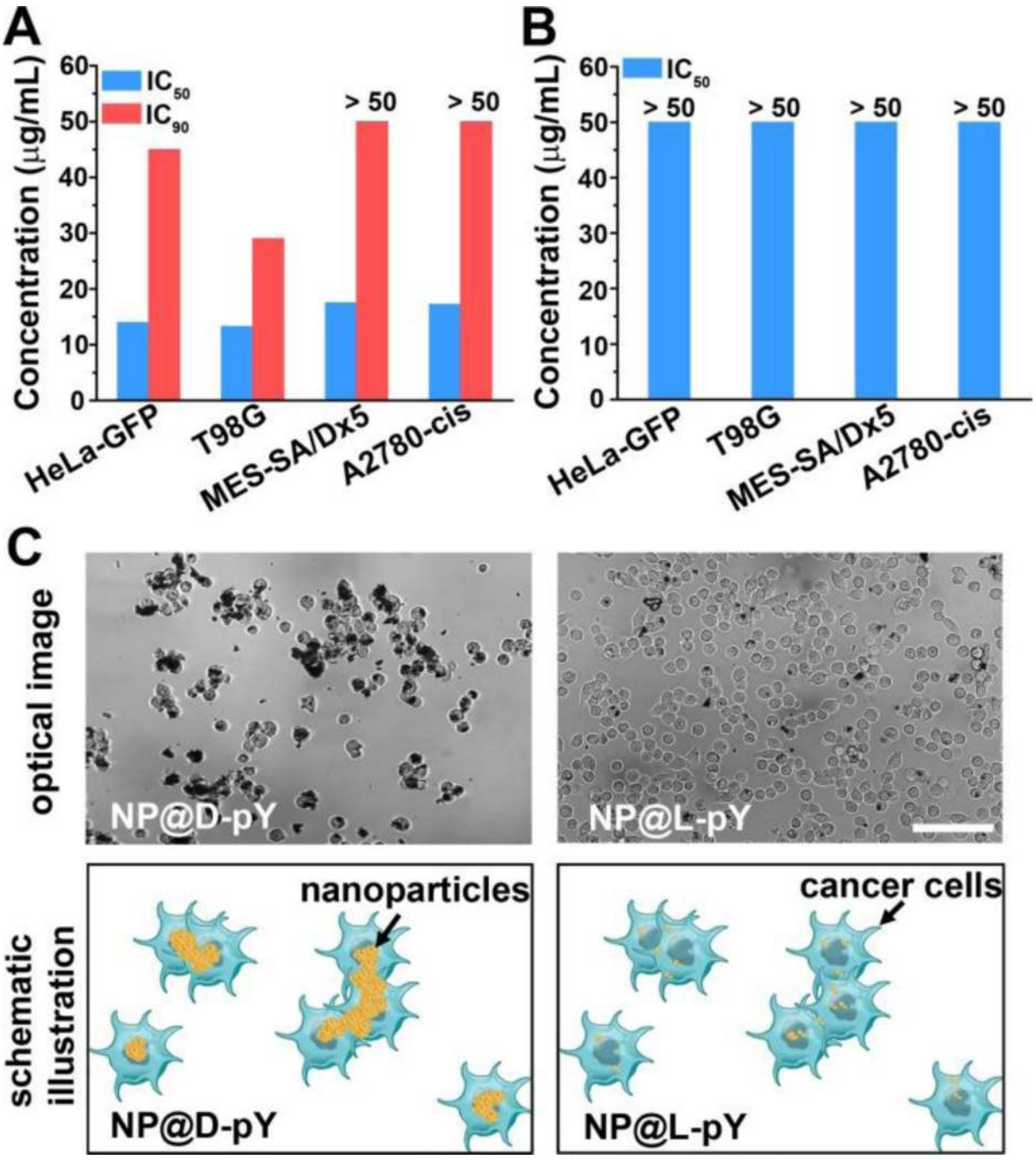

Figure 2.

(A) IC_{50} and/or IC_{90} of NP@D-pYs and (B) IC_{50} of NP@L-pYs against HeLa-GFP, T98G, MES-SA/Dx5, A2780-cis cells at 72 h. (C) The bright field microscope images (top panel) and their corresponding schematic illustration (bottom panel) of HeLa-GFP cells incubated with NP@D-pYs (left) and NP@L-pYs (right). The scale bar is 100 μm.

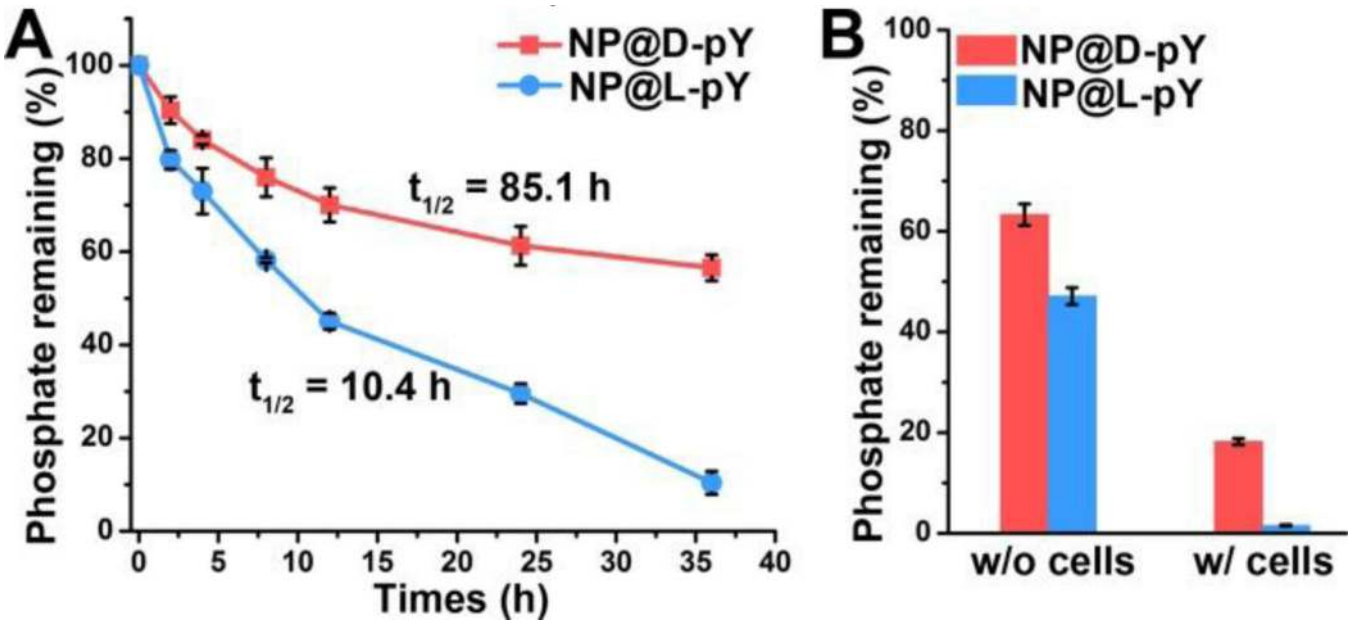

Figure 3.

The amount of phosphate molecules remains on NP@D-pYs and NP@L-pYs, respectively, after incubated with (A) conditioned culture medium (from 24 h culture of HeLa-GFP cells); (B) conditioned medium without or with HeLa-GFP cells at 12 h.

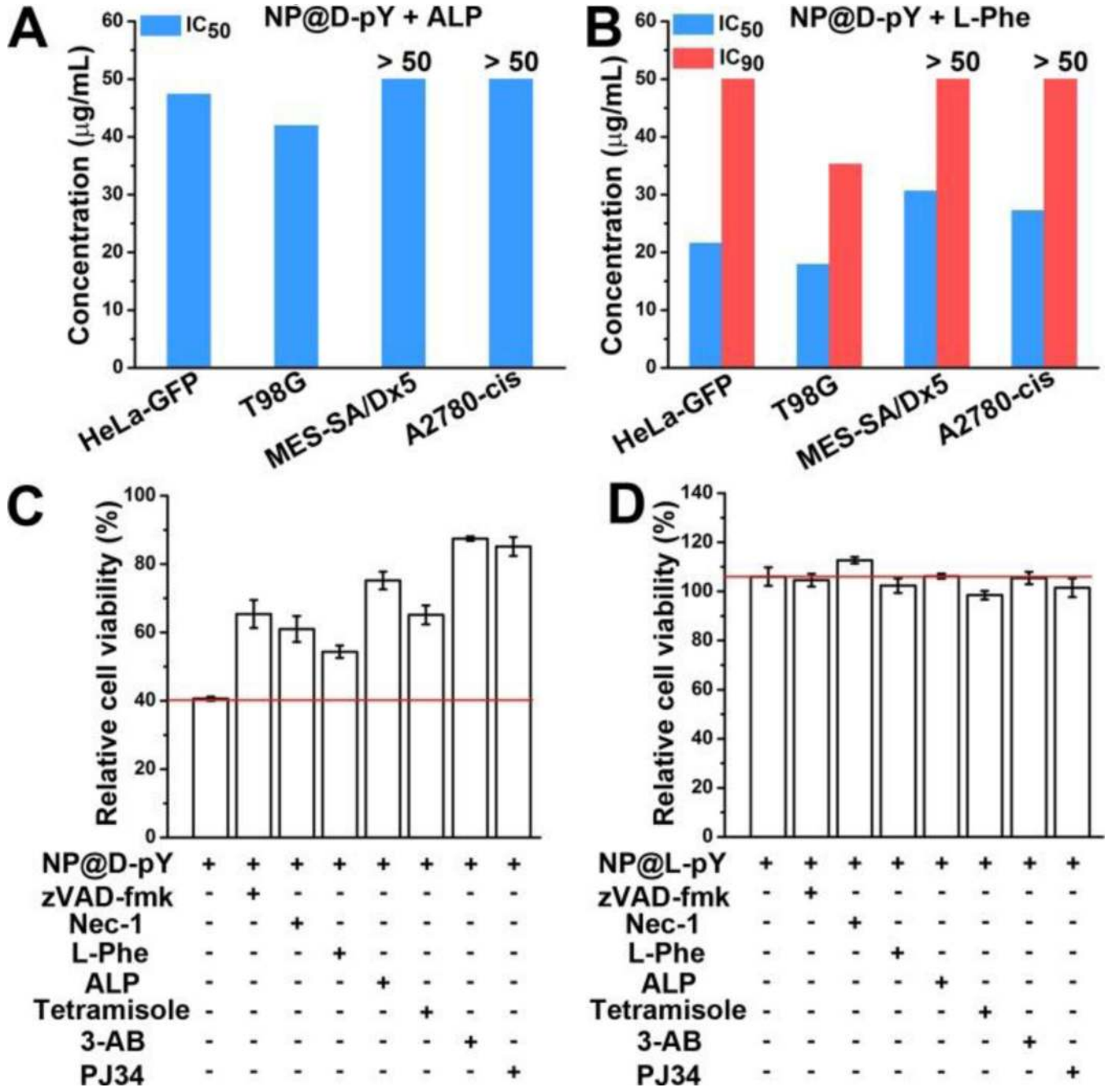

Figure 4.

IC_{50} and/or IC_{90} of NP@D-pY co-incubated with (A) 5U/mL ALP and (B) 5 mM L-Phe against HeLa-GFP, T98G, MES-SA/Dx5, A2780-cis cells at 72 h. Cell viability (determined by MTT assay) of HeLa-GFP cells incubated with (C) NP@D-pY and (D) NP@L-pY in the presence of several inhibitors (e.g., zVAD-fmk, necrostatin-1, L-Phe, ALP, tetramisole, 3-Aminobenzamide, or PJ34) at 48 h.

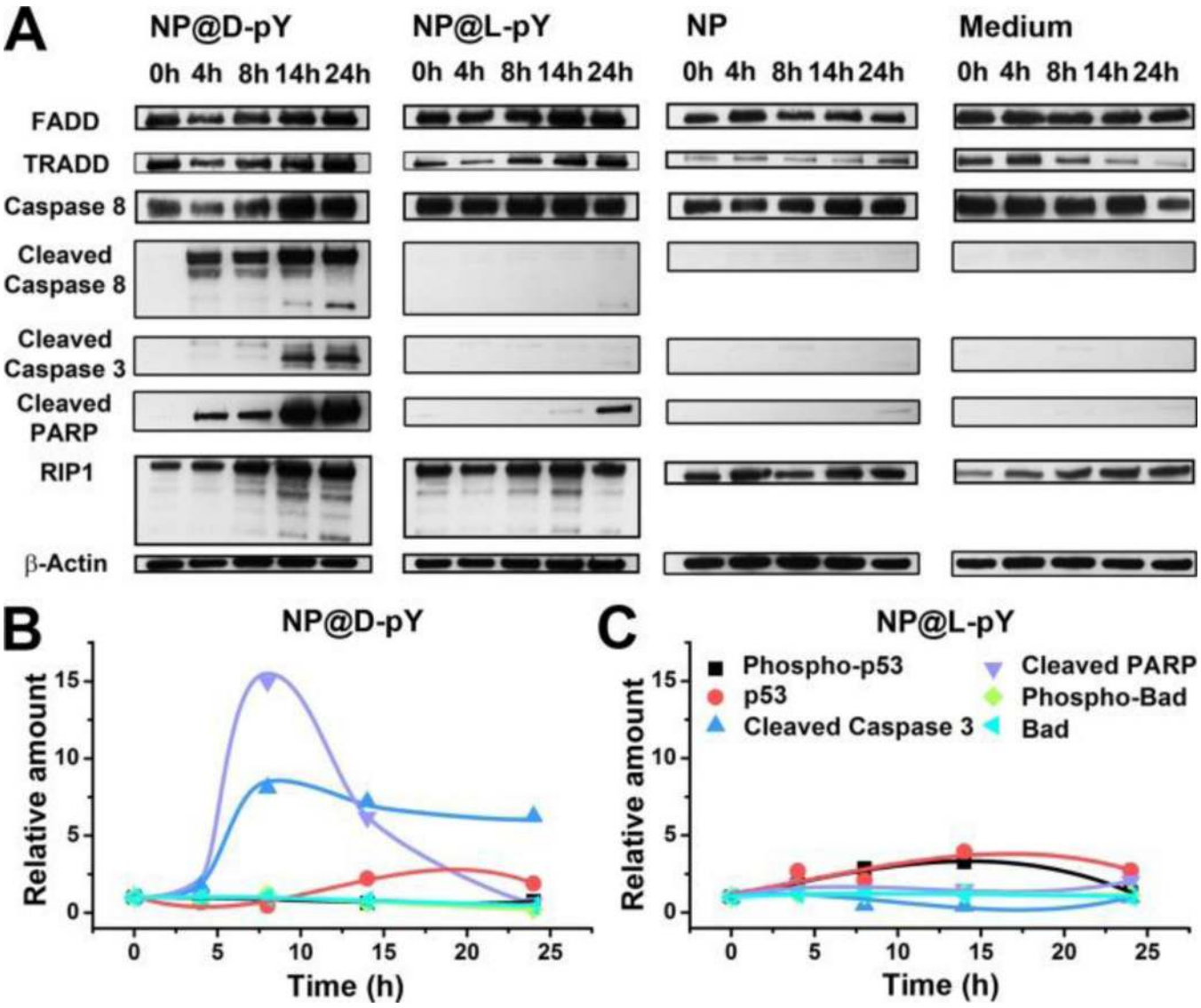

Figure 5.

(A) Western blot analysis shows change of cell death signaling molecules over time in HeLa-GFP cells treated by NP@D-pYs, NP@L-pYs, NP, and in normal growth medium. Change of relative amount of apoptosis signaling molecules over time in HeLa-GFP cells treated by (B) NP@D-pY or (C) NP@L-pY. All nanoparticle concentrations are 20 μg/mL.